THE EFFECT OF BLADE PITCH ANGLE ON THE AIRFLOW OF AXIAL FAN AT DIFFERENT OPERATIONAL CONDITIONS

Nguyen Duc Trung[1], Nguyen Truong Giang[1], Phan Minh Thuy[1], Nguyen Thi Thu Hien[1], Trinh Huu Truong[1], Vu Dinh Hieu[1], Thach Ngoc Mai[1], Nguyen Duc Nam[2], Nguyen Van Khuyen[3], Nguyen Trong Linh[3], Le Minh Toi[3], Nguyen Trung Hieu[4,*]

DOI: http://doi.org/ 10.57001/huih5804.2025.262

ABSTRACT

This study investigates the influence of blade pitch angle on airflow characteristics and efficiency of axial fans under various operational conditions using (CFD). By simulating airflow patterns across pitch angles ranging from 5° to 70° at different rotational speeds and load scenarios, we identify optimal configurations that enhance aerodynamic performance. The results indicate that pitch angles between 30° and 40° consistently yield the highest airflow rates. Furthermore, the effect of pitch angle diminishes as the system load increases, underscoring the importance of load-specific optimization. This work provides practical insights for fan design in HVAC and industrial applications.

Keywords: *Axial fan, CFD simulation, pitch angle variation, over load operation.*

[1]School of Chemistry and Life Sciences, Hanoi University of Science and Technology, Vietnam

[2]School of Electrical & Electronics Engineering, Hanoi University of Industry, Vietnam

[3]Department of R&D, Hanoi Mechanical Electric Group, JSC, Vietnam

[4]School of Materials, Hanoi University of Science and Technology, Vietnam

[*]Email: hieu.nguyentrung@hust.edu.vn

Received: 02/6/2025

Revised: 07/7/2025

Accepted: 25/7/2025

1. INTRODUCTION

Axial fans are essential components in ventilation, cooling, and HVAC systems due to their ability to deliver high airflow rates with low energy consumption [1, 2]. The blade pitch angle, a critical design parameter, significantly affects the airflow capacity and energy efficiency of the fan [3, 4]. Studies have shown that an optimal blade pitch angle, typically ranging from 30° to 45°, yields the highest performance under various operating conditions [5]. Specifically, it is demonstrated that precise adjustment of the blade angle can enhance energy efficiency by up to 3%, a particularly important factor in energy-intensive industrial applications such as manufacturing plants or data centers [5]. Furthermore, a research emphasized that the optimal blade angle depends not only on the rotational speed but also on static pressure conditions and the aerodynamic characteristics of the blade profile, thereby highlighting the necessity of application-specific design optimization [6].

From another perspective, in fan system design, the load must be tailored to the intended application. The duct resistance of the load directly impacts the airflow rate of axial fans: the larger the load, the greater the duct resistance, leading to a decrease in airflow [7, 8]. In this study, the airflow characteristics of a pneumatic conveying system driven by an axial fan will be simulated under different load conditions. Additionally, a comprehensive assessment will be conducted on the influence of blade pitch angle on airflow rate and fan efficiency under various operating conditions, considering different load levels and fan rotational speeds.

This study employs CFD simulations to determine the optimal blade pitch angle for axial fan designs at various rotational speeds. CFD simulations, conducted using software such as ANSYS Fluent, enable detailed analysis of airflow and pressure patterns while significantly reducing costs and time compared to traditional physical testing [9, 10]. The simulation results indicate that adjusting the blade pitch angle not only improves the airflow rate but also reduces flow separation, thereby enhancing the overall performance of the fan [11]. This

approach is particularly effective for optimizing axial fan performance in practical applications such as HVAC systems, industrial ventilation, and aerospace engineering, where high energy efficiency and adaptability to varying operating conditions are critically required.

2. METHODOLOGY

2.1. Theoretical basis

The Navier - Stokes equations constitute the fundamental framework of fluid dynamics, governing the conservation of mass and momentum in both of incompressible and compressible fluid flows.

$$\rho\left(\frac{\partial u}{\partial t}+u.\nabla u\right)=-\nabla p+\nabla.(\mu.\nabla u)+F \quad (1)$$

These equations describe the motion of fluid through a set of coupled, nonlinear partial differential equations (PDEs), where the primary variables include fluid density (ρ, kg/m^3), velocity vector (u, m/s), pressure (p, Pa), and dynamic viscosity (μ, Pa.s). The mathematical form of these equations varies with specific boundary conditions, which depend on the flow domain geometry, initial states, and external forces.

Due to the complexity of these equations and the intricate boundary conditions present in real-world applications, exact analytical solutions are generally unattainable. Consequently, numerical techniques within the framework of CFD have become the standard approach for solving such systems. In contemporary CFD practice, the Navier–Stokes equations are typically discretized using methods such as the Finite Difference Method (FDM), Finite Element Method (FEM), or Finite Volume Method (FVM).

In this study, the Finite Volume Method was employed using ANSYS Fluent (version 19.2) to simulate the internal airflow through an axial fan under varying operational scenarios. To accurately resolve the effects of turbulence, the realizable k-ε turbulence model was adopted, which provides robust predictions of turbulent kinetic energy and dissipation rate, especially in regions near walls and flow separations [12, 13]. This modeling strategy enables reliable and efficient simulation of the complex flow fields associated with rotating machinery such as axial fans [14].

2.2. Parameters of axial and different load conditions

The axial fan whose dimension are shown in Table 1 and aerodynamically shaped blades which is illustrated in Fig. 1 is tested at three different values of rotational speed at: 270rpm, 216rpm and 162rpm. The investigated fan in this study was designed, tested, manufactured and commercialized by Hanoi Mechanical Electric Group, JSC.

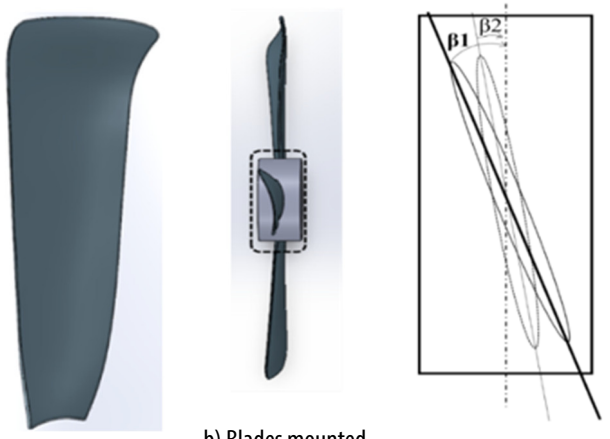

a) Blade profile b) Blades mounted on rotor c) Variable pitch angle

Fig. 1. Description of pitch angle on axial fan

The fan blades also can vary pitch angle (β) synchronously from 5° to 70°. The complete geometry was modeled using SolidWorks 2022 and incorporated into the CFD workflow.

Table 1. Basic dimensions of the fan

Symbol	*D*	D_t	D_{tr}	A
Description	Fan casing diameter	Hub diameter	Shaft diameter	Casing width
Dimension (mm)	1400	1300	250	200

The diagram of the whole system is shown in Fig. 2 for three different load conditons.

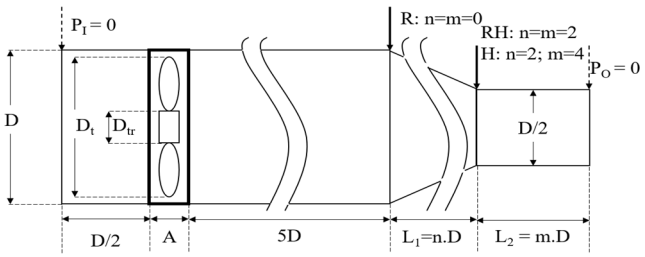

Fig. 2. Axial fan model with different loads

Three representative configurations were developed: an rated load (R: n = m = 0), rather heavy load (RH: n = m = 2) and a heavy load (H: n = 2, m = 4). These configurations are illustrated in Fig. 2.

The simulation results allow to find the pitch angle which maximizes airflow (β_{max}) at different load condition and with different rotational speeds.

2.3. Boundary condition and mesh setting

To investigate the aerodynamic performance of the axial fan, numerical simulations were conducted using

ANSYS Fluent, version 19.2. This software employs the FVM to discretize and solve the Reynolds-Averaged Navier-Stokes (RANS) equations, which govern the behavior of turbulent, incompressible flow. Integrated turbulence modeling is essential for capturing complex flow structures within and downstream of rotating machinery. In this study, the k–ω shear stress transport (SST) turbulence model was selected due to its superior capability in resolving near-wall flow behavior and predicting flow separation, which are critical to the accurate representation of fan blade aerodynamics.

The fan's rotational motion was modeled using the Moving Reference Frame (MRF) approach, which allows steady-state simulation of rotating components while maintaining computational efficiency. Boundary conditions were defined as follows: gauge pressure on both of inlet and outlet surface were set to 0 Pa (Fig. 2), the walls were treated with no-slip conditions. These boundary conditions approximate standard operating conditions under atmospheric pressure and are suitable for evaluating relative pressure and velocity distributions within the fan domain.

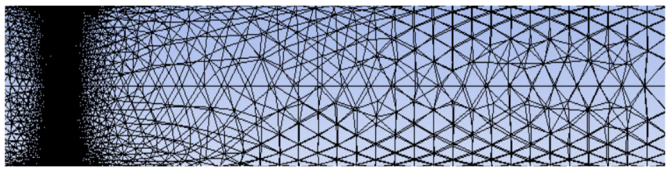

Fig. 3. Computational mesh topology on the blade

Mesh generation directly affects the simulation results. A coarse mesh may result in a loss of flow details, reducing accuracy and potentially missing phenomena such as vortices. On the other hand, a very fine mesh can significantly increase computational time and cause numerical instability if convergence parameters are not properly controlled. The mesh quality metrics such as Skewness were applied. The mesh was generated based on the models described above and is illustrated in Fig. 3. The grid density is specially intensified in curvy area of the blade by tuning experience.

3. RESULTS AND DISCUSSION

3.1 Rated load condition

Table 2 presents the variation of airflow rate (F, kg/s) as a function of pitch angle (β) across three different rotor speeds for the case of rated load condition.

The results show that the airflow of the axial fan depends on both the blade pitch angle and the rotational speed. Initially, with a pitch angle increment of 5°, the maximum airflow region was identified to lie between 35° and 40°. Upon further investigation using a finer increment of 2.5°, the peak region was more precisely determined to be around 37.5°. As β increases from 5° to approximately 37.5°, the airflow gradually increases at all three speeds because the increase in β enhances the thrust on the air, thereby increasing the airflow. From a pitch angle of 37.5° and above, the airflow begins to decrease consistently across all three fan rotational speeds.

However, further increases in the pitch angle lead to significant flow turbulence, which reduces the airflow. This demonstrates that in axial fan designs, it is essential to select the optimal blade pitch angle to achieve maximum airflow, especially when operating under varying conditions.

The results above indicate a relatively significant variation in airflow of the axial fan with different pitch angles at rated load condition.

Table 2. Airflow due to pitch angle at different rotational speeds with rated load (R)

N_1= 270 (rpm)				N_2= 216 (rpm)				N_3= 162 (rpm)			
β(°)	F(kg/s)	β(°)	F(kg/s)	β(°)	F(kg/s)	β(°)	F(kg/s)	β(°)	F(kg/s)	β(°)	F(kg/s)
5.0	4.237	40.0	7.538	05.0	3.224	40.0	5.968	05.0	2.295	40.0	4.485
10.0	5.278	45.0	7.291	10.0	4.129	45.0	5.893	10.0	3.159	45.0	4.368
15.0	6.096	50.0	6.925	15.0	4.855	50.0	5.507	15.0	3.626	50.0	4.109
20.0	6.708	55.0	5.629	20.0	5.347	55.0	4.478	20.0	3.990	55.0	3.278
25.0	7.124	60.0	4.893	25.0	5.688	60.0	4.015	25.0	4.243	60.0	2.906
30.0	7.393	65.0	4.687	30.0	5.891	65.0	3.761	30.0	4.397	65.0	2.870
35.0	7.595	70.0	4.513	35.0	6.026	70.0	3.309	35.0	4.482	70.0	2.452
37.5	7.585			37.5	6.013			37.5	4.485		

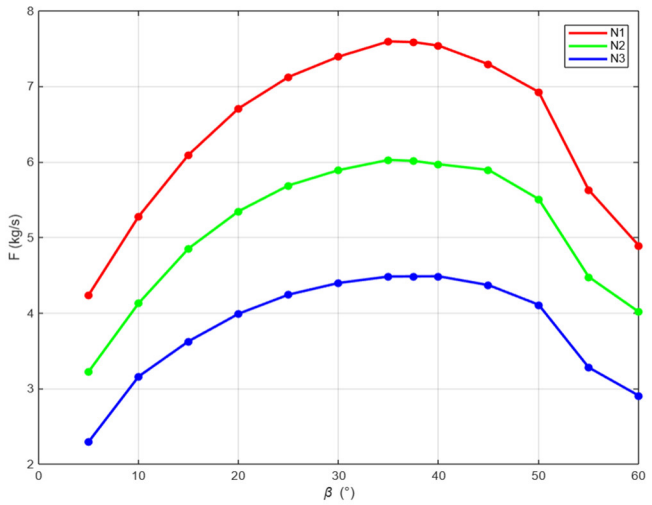

Fig. 4. Airflow - Pitch angle graph for the case of rated load condition

The simulation results for the axial fan with rated load condition demonstrate a consistent trend in airflow behaviour as a function β. In all cases, the airflow initially increases with the pitch angle, reaches a maximum, and subsequently decreases, forming a bell-shaped curve across the pitch angle spectrum, this result is also consistent with the simulation results previous study [5]. This curve shape reflects the aerodynamic characteristics of the fan blades: when the pitch angle approaches 0°, the blades primarily generate strong suction but weak thrust, resulting in low airflow. Conversely, as the pitch angle approaches 90°, the blades predominantly produce thrust in a direction perpendicular to the rotation axis; however, aerodynamic efficiency significantly decreases due to flow separation and energy losses, which in turn leads to a reduction in airflow.

3.2. Rather heavy load and heavy load conditions

Table 3 and Table 4 present the variation of airflow rate (F, kg/s) as a function of pitch angle (β) across three different rotor speeds for the case of rather heavy load condition (RH) and heavy load condition (H).

Fig. 5 is constructed to illustrate the dependence of airflow on the pitch angle from Table 3 and Table 4. Based on the results from the table and the graphs (solid line) for RH, it can be observed that as β increases from 0° to approximately 40° - 42.5°, the airflow gradually increases. However, beyond a pitch angle of around 42.5°, the airflow begins to decline. Furthermore, a closer examination of the graphs reveals that as the fan rotational speed decreases, β_{max} occurs tends to slightly decrease as well.

From the table, a graph (dashed line) can be derived to illustrate the relationship between airflow and blade pitch angle with heavy load conditions. In the simulation of airflow through the axial fan with heavy load conditions, it was observed that the airflow increases as β rises from 0° to 30°, and begins to decrease from 30° onwards.

Table 3. Airflow due to pitch angle at different rotational speeds with rather heavy load (RH)

N_1= 270 (rpm)				N_2= 216 (rpm)				N_3= 162 (rpm)			
β(°)	F(kg/s)	β(°)	F(kg/s)	β(°)	F(kg/s)	β(°)	F(kg/s)	β(°)	F(kg/s)	β(°)	F(kg/s)
10.0	1.620	40.0	1.759	10.0	1.339	40.0	1.407	10.0	0.994	40.0	1.066
20.0	1.684	42.5	1.772	20.0	1.349	42.5	1.419	20.0	1.047	42.5	1.060
30.0	1.712	50.0	1.685	30.0	1.385	50.0	1.348	30.0	1.063	50.0	1.004
35.0	1.693	60.0	1.693	35.0	1.365	60.0	1.328	35.0	1.016	60.0	0.992
37.5	1.703	70.0	1.447	37.5	1.357	70.0	1.208	37.5	1.028	70.0	0.891

Table 4. Airflow due to pitch angle at different rotational speeds with heavy load (H)

N_1= 270 (rpm)				N_2= 216 (rpm)				N_3= 162 (rpm)			
β(°)	F(kg/s)	β(°)	F(kg/s)	β(°)	F(kg/s)	β(°)	F(kg/s)	β(°)	F(kg/s)	β(°)	F(kg/s)
10.0	1.642	35.0	1.806	10.0	1.344	35.0	1.439	10.0	1.002	35.0	1.078
20.0	1.806	40.0	1.826	20.0	1.440	40.0	1.449	20.0	1.078	40.0	1.080
27.5	1.813	50.0	1.712	27.5	1.454	50.0	1.372	27.5	1.090	50.0	1.035
30.0	1.833	60.0	1.728	30.0	1.463	60.0	1.388	30.0	1.099	60.0	1.044
32.5	1.704	70.0	1.512	32.5	1.367	70.0	1.223	32.5	1.027	70.0	0.925

The analysis with rather heavy load and heavy load further confirms the influence of pitch angle on the airflow rate in axial fans. The range of pitch angles that yields the maximum airflow rate lies between 30° and 40°. However, as the load increases, the effect of pitch angle on the airflow rate diminishes. Therefore, adjusting β to control airflow is more practically significant for no-load axial fan operation. Additionally, as the axial fan load increases, the pitch angle range corresponding to the maximum airflow tends to shift downward - for instance, with rather heavy load, it approaches 40°, while with heavy load, it tends toward 30°.

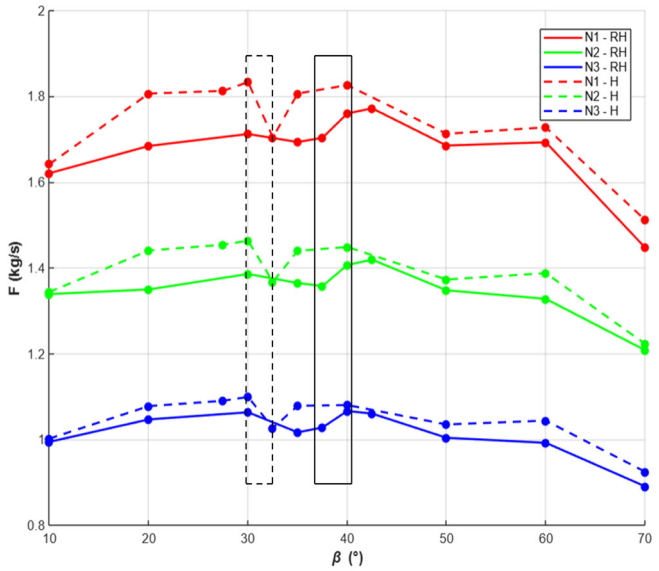

Fig. 5. Airflow - Pitch angle graph for the case of RH and H

Based on the Fig. 4 and Fig. 5 illustrating airflow with different load conditions, it is observed that: with R and H, β_{max} hardly depend on rotor angular speed. However, with RH, the rotational speed exhibits a slight influence. Specifically, at a rather heavy load, when the fan speeds are 270rpm and 216rpm, β_{max} is 42.5°. In contrast, at a lower speed of 162rpm, β_{max} decreases to 40°.

When simulating airflow with heavy load conditions (RH and H), a region of distinctive sensitiveness was observed, characterized by the presence of a local minimum. In this region, with a pitch angle increment of 2.5°, the transition between the peak point and the local minimum is very steep. Moreover, the slope at this extra ordinary range becomes steeper for heavier load and bigger rotational speed. This sharp drop may be attributed to blade flexibility or deformation, leading to aerodynamic instability. Therefore, special attention should be given to this sensitive range during the design of axial fans to ensure stable performance.

4. CONCLUSION

CFD method based on ANSYS allows to saves time, effort and cost in design process by system operation simulation. The tuning of blade profile, blade pitch angle and various parameters of axial fan can be computerized simply, quickly and easily.

In the design process, it is essential to optimize factors that directly influence airflow, including the blade pitch angle. This study demonstrates that there always exists a specific pitch angle at which the airflow reaches its maximum with different load conditions. Furthermore, the study reveals that as the fan load increases, the range of pitch angles that produces maximum airflow tends to decrease. By simulating airflow through the axial fan model with the selected blade profile, the optimal pitch angle was determined to lie within the range of 30° to 40°. The result of this study proposed the manufacturer the permitted range for pitch angle tuning.

As a result, adjusting pitch angle is fully significant for airflow regulation with lighter load than rated condition because of the extra ordinary range appearance with heavier load.

REFERENCES

[1]. Yang J., Wu J., Xian T., Zhang H., Li X., "Research on energy-saving optimization of commercial central air-conditioning based on data mining algorithm," *Energy Build*, 272, 112326, 2022.

[2]. Gao Z., Yu J., Zhao A., Hu Q., Yang S., "A hybrid method of cooling load forecasting for large commercial building based on extreme learning machine," *Energy*, 238, 122073, 2022.

[3]. Liu S.H., Huang R.F., Chen L.J., "Performance and inter-blade flow of axial flow fans with different blade angles of attack," *J Chin Inst Eng A,* 34/1, 141-153, 2011.

[4]. Ye X., Fan F., Zhang R., Li C., "Prediction of performance of a variable-pitch axial fan with forward-skewed blades," *Energies*, 12/12, Article 2353, 2019.

[5]. Jeon S.T., Cho J.P., "Effect of pitch angle and blade length on an axial flow fan performance," *J Korea Acad-Ind Coop Soc*, 14/7, 3170-3176, 2013.

[6]. Kim Y.J., Kim L.Y.H., "erformance Enhancement of Axial Fan Blade through Multi-Objective Optimization Techniques," *Journal of Mechanical Science and Technology*, 24. 2059-2066, 2010.

[7]. Onder M., Sarac S., Cevik E., "The influence of ventilation variables on the volume rate of airflow delivered to the face of long drivages," *Tunn Undergr Space Technol*, 21/5, 568-574, 2006.

[8]. Patel J.S., Patel S.M., "Parameter affecting the performance of axial fan performance," *Int J Eng Res Technol*., 1, 3, 2012.

[9]. Cheteu L.H.K., Dou H.S., "Analysis and simulation of axial fan using CFD," *Int J Mech Ind Technol,* 9, 11-17, 2021.

[10]. ANSYS, *ANSYS Fluent theory guide: Computational fluid dynamics modeling of rotating machinery*. 2021

[11]. Lee C., Choi J., Hwang J., Lee H., Lee S., Yang S.H., "Optimal design of a variable-pitch axial flow fan by applying optimization algorithm to design, through-flow analysis and CFD simulation methods," in *Proc Int Conf Simul Model Methodol Technol Appl,* 363-369, 2024.

[12]. Wilcox D.C., *Turbulence Modeling for CFD,* Second edition. Anaheim: DCW Industries, p. 174, 1998.

[13] Bacak A., Pınarbaşı A., "Numerical investigation of acoustics performance of low-pressure ducted axial fan by using different turbulence models," in *ITM Web of Conferences*, 22, Article 01004, 2018.

[14]. Liu R., Xu S., Sun K., Ju X., Zhang W., Wang W., Ma X., Pan Y., Li J., Ren G., "CFD analysis and optimization of axial flow fans," *International Journal for Simulation and Multidisciplinary Design Optimization*, 15, Article 11, 2024.